




## Linear polar molecule in a two-color cw laser field: A symmetry analysis

David Mellado-Alcedo <sup>1</sup>, Niurka R. Quintero <sup>2</sup>, and Rosario González-Férez <sup>1</sup>

<sup>1</sup>*Instituto Carlos I de Física Teórica y Computacional, and Departamento de Física Atómica, Molecular y Nuclear, Universidad de Granada, 18071 Granada, Spain*

<sup>2</sup>*Departamento de Física Aplicada I, Universidad de Sevilla, 41011 Sevilla, Spain*



(Received 15 January 2020; revised 25 April 2020; accepted 1 July 2020; published 10 August 2020)

A theoretical study of the rotational dynamics of a linear polar molecule in a two-color nonresonant cw laser field is presented. By systematically considering the interactions of this field with the electric dipole moment, polarizability, and hyperpolarizability of the molecule, the implications that the symmetries of the Hamiltonian have on the rotational dynamics are explored in a regime where the time-average approximation does not hold. It is shown that the alignment and orientation satisfy certain symmetries as functions of the phases and field strengths, and that they can be expressed as analytic functions in terms of these main parameters of the two-color laser field.

DOI: [10.1103/PhysRevA.102.023110](https://doi.org/10.1103/PhysRevA.102.023110)

### I. INTRODUCTION

Biharmonic signals are widely used in many areas of physics in order to break the time-shift symmetry of the external forces and of the electromagnetic fields [1–6]. This symmetry breaking induces a plethora of unexpected phenomena, as, for example, the dissipation-induced net motion, the current reversals by increasing the amplitudes, and resonances as a function of the frequency and of the damping coefficient [7,8]. These phenomena have been observed in seemingly unrelated systems, such as semiconductors [9], Josephson junctions [10], optical lattices [11], ferrofluids [12], Brownian particles [2], Bose-Einstein condensates [13], or solitons in nonlinear systems [14–16]. Recent studies show that, regardless of the system, the symmetries of the biharmonic force determine the dependence of the measurements on the amplitudes and phases of this biharmonic force [17–19].

The spherical symmetry of a thermal sample of molecules is broken by inducing orientation and alignment [20–25] with experimental techniques such as brute force orientation [26–28], combined electrostatic and nonresonant laser fields [29–35], THz pulses [36–41], or the phase-locked two-color laser field [42–46]. An aligned molecule is characterized by the confinement of the molecular fixed axes along the laboratory fixed frame, and keeping the head-versus-tail symmetry [25]. For an oriented molecule, this symmetry is broken and the dipole moment is pointing towards one hemisphere rather than the opposite [20,24]. In the spirit of biharmonic signals, continuous-wave (cw) nonresonant laser fields could be employed to create directional states of polar molecules, rather than the laser pulses used in experiments, the time envelope of which is often given by a Gaussian function.

In this paper, a linear polar molecule in a two-color continuous-wave nonresonant laser field is considered. Within the Born-Oppenheimer and the rigid-rotor approximations, the field-dressed rotational dynamics is analyzed. The laser frequency is chosen so that the time-average approximation [47] is not correct. The validity of this approximation is

investigated in Appendix A. Here, it is assumed that no electronic, vibrational, or rotational transitions are driven by this field. A systematic and detailed analysis of the implications that the symmetries of the Hamiltonian have in the field-dressed rotational dynamics is presented. By gradually including the interactions of the field with the electric dipole moment, polarizability, and hyperpolarizability in the description, the effect of these symmetries is analyzed, and the identities that the expectation values describing the field-dressed rotational dynamics satisfy are derived. Due to these symmetries, it is shown that for a fixed propagation time the alignment and orientation can be expressed as analytic functions that depend on the amplitudes and phases of the harmonics appearing on the Hamiltonian. Furthermore, only a few coefficients significantly contribute to the series expansion, and they have been obtained. In addition, it is shown analytically that it is not possible to orient on average a polar molecule with a one-color cw laser field being necessary a two-color one. The sum of the two frequencies of this two-color laser should be an odd multiple of the main frequency. Here, the carbonyl sulfide molecule OCS serves as a prototype system to present and discuss these results.

### II. THE HAMILTONIAN AND THE SYMMETRIES

A linear polar molecule exposed to a phase-controlled cw two-color laser field linearly polarized along the laboratory fixed frame (LFF)  $Z$  axis is considered. The corresponding electric field  $\mathbf{E}(t) = E(t)\mathbf{Z}$  is given by the biharmonic function

$$E(t) = \sum_{i=1,2} \epsilon_i \cos[q_i \omega(t + t_0) + \delta_i], \quad (1)$$

with  $q_i \omega$ ,  $\epsilon_i$ , and  $\delta_i$  being the laser frequency, electric-field strength, and phase of the  $i$ th harmonic, respectively, and with  $q_i$  a positive integer. The time shift between the turning on of the two-color laser field and the instant when the molecule starts to interact with it is  $t_0$ .

The molecule is described by the Born-Oppenheimer approximation, and the rotational motion is investigated using the rigid rotor approach. Within this framework, the field-dressed rotational Hamiltonian is given by [48,49]

$$H = H_0 + H_\mu + H_\alpha + H_\beta, \quad (2)$$

where the first term stands for the field-free Hamiltonian:

$$H_0 = B\mathbf{J}^2, \quad (3)$$

with  $B$  being the rotational constant of the molecule, and  $\mathbf{J}$  the rotational angular momentum operator. The second, third, and fourth terms represent the interaction of the electric field with the electric dipole moment, polarizability, and hyperpolarizability of the molecule, respectively:

$$H_\mu = -\mu \cos \theta E(t), \quad (4)$$

$$H_\alpha = -\frac{1}{2}\Delta\alpha \cos^2 \theta E^2(t), \quad (5)$$

$$H_\beta = -\frac{1}{6}(\Delta\beta \cos^3 \theta + 3\beta_\perp \cos \theta)E^3(t). \quad (6)$$

In these expressions,  $\theta$  is the Euler angle between the internuclear molecular axis and the LFF  $Z$  axis,  $\mu$  is the permanent electric dipole moment,  $\Delta\alpha = \alpha_\parallel - \alpha_\perp$  is the polarizability anisotropy with  $\alpha_\perp$  and  $\alpha_\parallel$  being its perpendicular and parallel components, and  $\Delta\beta = \beta_\parallel - 3\beta_\perp$  is the hyperpolarizability anisotropy with  $\beta_\perp$  and  $\beta_\parallel$  being the perpendicular and parallel components, respectively.

The symmetry operations for polar linear molecules are those from the  $C_{\infty v}$  point group. Since the operator  $\mathbf{J}^2$  is invariant under arbitrary rotations, the field-free rigid rotor Hamiltonian (3) belongs to the  $SO(3)$  group. The field-dressed Hamiltonian (2) is invariant under any rotation of an arbitrary angle  $\chi$  around the LFF  $Z$  axis,  $C_Z(\chi)$ , and reflections in any plane containing this  $Z$  axis. These symmetries imply that the projection of the rotational angular momentum along the LFF  $Z$  axis,  $M$ , is a good quantum number, and that the rotational dynamics of the states with  $M$  and  $-M$  shares many properties, for instance, the energy, orientation, and alignment.

The time-dependent Schrödinger equation associated to the Hamiltonian (2) is numerically solved assuming that the time-average approximation is not correct (see Appendix A). The computational technique combines the short iterative Lanczos method [50] for the time variable, and a basis set expansion in terms of linear combinations of spherical harmonics  $Y_{J,M}(\Omega)$ , with  $\Omega = (\theta, \phi)$  being the Euler angles. These linear combinations are constructed to satisfy the spatial symmetries of the Hamiltonian. The field-dressed rotational dynamics is analyzed in terms of the expectation value:

$$\langle \cos^k \theta \rangle = \int \psi^*(\Omega, t) \cos^k \theta \psi(\Omega, t) d\Omega, \quad (7)$$

with  $\psi(\Omega, t)$  being the time-dependent wave function, and  $k \in \mathbb{Z}^+$ . For the orientation and alignment,  $k = 1$  and 2, respectively.

The two-color electric field (1) is invariant under the transformation

$$\mathcal{T} : (q_1, q_2, \omega) \rightarrow \left( \kappa q_1, \kappa q_2, \frac{\omega}{\kappa} \right) \quad \text{with } \kappa \in \mathbb{Z}^+, \quad (8)$$

and, therefore, the Hamiltonian (2) is also invariant under this transformation. Thus, the analysis can be restricted to  $q_1$  and  $q_2$  satisfying  $\text{gcd}(q_1, q_2) = 1$ . The symmetries in the phases  $\delta_1$  and  $\delta_2$ , and in the amplitudes  $\epsilon_1$  and  $\epsilon_2$  of the two-color electric field (1), imply that

$$\begin{aligned} \langle \cos^k \theta \rangle(t, t_0, \epsilon_1, \epsilon_2, \delta_1, \delta_2) \\ = \langle \cos^k \theta \rangle(t, t_0, (-1)^{n_1} \epsilon_1, (-1)^{n_2} \epsilon_2, \delta_1 + n_1 \pi, \delta_2 + n_2 \pi), \end{aligned} \quad (9)$$

with  $n_1$  and  $n_2$  being integers. This expression shows explicitly the dependence on  $t, t_0, \epsilon_1, \epsilon_2, \delta_1$ , and  $\delta_2$  of this expectation value. The inversion of the electric-field direction gives rise to the following invariance:

$$\begin{aligned} \langle \cos^k \theta \rangle(t, t_0, \epsilon_1, \epsilon_2, \delta_1, \delta_2) \\ = (-1)^k \langle \cos^k \theta \rangle(t, t_0, -\epsilon_1, -\epsilon_2, \delta_1, \delta_2). \end{aligned} \quad (10)$$

The Hamiltonian (2) is invariant under a shift in  $t_0$  by changing the phases  $\delta_1$  and  $\delta_2$ , and it holds that

$$\begin{aligned} \langle \cos^k \theta \rangle(t, t_0, \epsilon_1, \epsilon_2, \delta_1, \delta_2) \\ = \langle \cos^k \theta \rangle(t, t_0 + \tau, \epsilon_1, \epsilon_2, \delta_1 - q_1 \omega \tau, \delta_2 - q_2 \omega \tau) \quad \forall \tau. \end{aligned} \quad (11)$$

The invariance of the Hamiltonian (2) under a simultaneous inversion of  $t, t_0, \delta_1$ , and  $\delta_2$  implies that

$$\begin{aligned} \langle \cos^k \theta \rangle(t, t_0, \epsilon_1, \epsilon_2, \delta_1, \delta_2) \\ = \langle \cos^k \theta \rangle(-t, -t_0, \epsilon_1, \epsilon_2, -\delta_1, -\delta_2). \end{aligned} \quad (12)$$

In contrast to other laser field parameters, the value of  $t_0$  cannot be easily controlled in an experiment. Therefore, this expectation value is averaged over  $t_0$  [19] as

$$\langle \langle \cos^k \theta \rangle \rangle = \frac{\omega}{2\pi} \int_0^{\frac{2\pi}{\omega}} dt_0 \langle \cos^k \theta \rangle \quad \text{with } k \in \mathbb{Z}^+, \quad (13)$$

where the integral is restricted to an electric-field period due to the  $t_0$  periodicity of the electric field (1).

For a one-color electric field, i.e., either  $\epsilon_1 = 0$  or  $\epsilon_2 = 0$ , or  $q_1 = q_2$ , the Hamiltonian (2) fulfills the symmetry in  $t_0$   $H(\theta, t_0) = H(\pi - \theta, t_0 + \frac{\pi}{q_i \omega})$ , with  $i = 1$  or 2, and the expectation value satisfies

$$\langle \cos^k \theta \rangle \left( t_0 + \frac{\pi}{q_i \omega} \right) = (-1)^k \langle \cos^k \theta \rangle(t_0) \quad (14)$$

and, therefore,

$$\langle \langle \cos^k \theta \rangle \rangle = [1 + (-1)^k] \frac{q_i \omega}{2\pi} \int_0^{\frac{\pi}{q_i \omega}} dt_0 \langle \cos^k \theta \rangle, \quad (15)$$

where the dependence on the field parameters is omitted. For  $k = 1$ , relation (15) indicates that on average the molecule is not oriented by a one-color laser field, regardless of its frequency, even if the three interactions are taken into account. For a fixed  $t_0$ , the molecule is oriented, and at  $t_0 + \frac{\pi}{q_i \omega}$  it possesses the same orientation but in the opposite direction [see Eq. (14)]. As a consequence, we obtain  $\langle \langle \cos^k \theta \rangle \rangle = 0$ . For  $k = 2$ , Eq. (15) implies that the interval of integration in Eq. (13) can be reduced to  $0 \leq t_0 \leq \frac{\pi}{q_i \omega}$ .

From the symmetries in Eq. (9), the  $t_0$ -averaged expectation value satisfies

$$\begin{aligned} \langle\langle \cos^k \theta \rangle\rangle(t, \epsilon_1, \epsilon_2, \delta_1, \delta_2) \\ = \langle\langle \cos^k \theta \rangle\rangle(t, (-1)^{n_1} \epsilon_1, (-1)^{n_2} \epsilon_2, \delta_1 + n_1 \pi, \delta_2 + n_2 \pi), \end{aligned} \quad (16)$$

with  $n_1$  and  $n_2$  being integers. The symmetry due to the inversion of the electric-field direction (10) reads as

$$\begin{aligned} \langle\langle \cos^k \theta \rangle\rangle(t, \epsilon_1, \epsilon_2, \delta_1, \delta_2) \\ = (-1)^k \langle\langle \cos^k \theta \rangle\rangle(t, -\epsilon_1, -\epsilon_2, \delta_1, \delta_2). \end{aligned} \quad (17)$$

The invariance on  $t_0$  (11) gives rise to the following phase-shift symmetry:

$$\begin{aligned} \langle\langle \cos^k \theta \rangle\rangle(t, \epsilon_1, \epsilon_2, \delta_1, \delta_2) \\ = \langle\langle \cos^k \theta \rangle\rangle(t, \epsilon_1, \epsilon_2, \delta_1 + q_1 \Delta, \delta_2 + q_2 \Delta) \end{aligned} \quad (18)$$

with  $\Delta$  being an arbitrary phase shift. The symmetry (12) is transformed as

$$\begin{aligned} \langle\langle \cos^k \theta \rangle\rangle(t, \epsilon_1, \epsilon_2, \delta_1, \delta_2) \\ = \langle\langle \cos^k \theta \rangle\rangle(-t, \epsilon_1, \epsilon_2, -\delta_1, -\delta_2). \end{aligned} \quad (19)$$

Furthermore, the identities (16), (17), and (18) imply that Eq. (19) becomes

$$\begin{aligned} \langle\langle \cos^k \theta \rangle\rangle(t, \epsilon_1, \epsilon_2, \delta_{1,n}, \delta_{2,n}) \\ = (-1)^{kn} \langle\langle \cos^k \theta \rangle\rangle(-t, \epsilon_1, \epsilon_2, \delta_{1,n}, \delta_{2,n}), \end{aligned} \quad (20)$$

which is the time-reversal symmetry for the specific phases  $\delta_{1,n} = n\frac{\pi}{2} + q_1 \Delta$  and  $\delta_{2,n} = (n+1 \pm 1)\frac{\pi}{2} + q_2 \Delta$ , with  $n$  an integer.

The symmetries (16), (17), and (18) imply additional identities for the  $t_0$ -averaged expectation value. For  $q_1$  and  $q_2$  odd integers, and  $k$  odd, it yields

$$\langle\langle \cos^k \theta \rangle\rangle(t, \epsilon_1, \epsilon_2, \delta_1, \delta_2) = 0, \quad (21)$$

which indicates the lack of orientation for  $k = 1$ , and for  $k$  even

$$\begin{aligned} \langle\langle \cos^k \theta \rangle\rangle(t, \epsilon_1, \epsilon_2, \delta_1, \delta_2) \\ = \langle\langle \cos^k \theta \rangle\rangle\left(t, \epsilon_1, \epsilon_2, \delta_1 + n_1 \frac{\pi}{2}, \delta_2 + [2 - (-1)^{\frac{q_2 - q_1}{2}}] n_1 \frac{\pi}{2}\right), \end{aligned} \quad (22)$$

with  $n_1$  being an integer. Thus, in this case the molecule is aligned but not oriented. For  $q_1$  odd and  $q_2$  even, it holds that

$$\begin{aligned} \langle\langle \cos^k \theta \rangle\rangle(t, \epsilon_1, \epsilon_2, \delta_1, \delta_2) \\ = (-1)^{k(\frac{n_1 q_2}{2} + n_2 q_1)} \langle\langle \cos^k \theta \rangle\rangle\left(t, \epsilon_1, \epsilon_2, \delta_1 + n_1 \frac{\pi}{2}, \delta_2 + n_2 \pi\right) \end{aligned} \quad (23)$$

with  $n_1$  and  $n_2$  being integers,  $k \in \mathbb{Z}^+$ , and the molecule is both oriented and aligned.

Most importantly, due to the symmetries of the Hamiltonian, for a fixed propagation time  $t$ , the  $t_0$ -averaged expectation value  $\langle\langle \cos^k \theta \rangle\rangle$  can be expressed as a series expansion in terms of the amplitude  $\epsilon_j$  and phase  $\delta_j$  of the  $j$  harmonics of the two-color electric field (1) [19]. These analytic functions

TABLE I. Relevant data for OCS [53].

$B$ ( $\text{cm}^{-1}$ )	$T_R$ (ps)	$\mu$ ( $D$ )	$\Delta\alpha$ (a.u.)	$\Delta\beta$ (a.u.)	$\beta_\perp$ (a.u.)
0.2029	82.2	0.71	27.26	132.3	-59.1

are derived in Appendix B [see Eqs. (B6), (B7), (B8), and (B9)].

### III. RESULTS

The carbonyl sulfide molecule OCS serves as a prototype for this paper; its data are summarized in Table I. The electric-field strengths are taken as  $\epsilon_1 = (1 - \gamma)E_0$  and  $\epsilon_2 = \gamma E_0$  with  $0 \leq \gamma \leq 1$ , and  $E_0 = \sqrt{\frac{2I}{c\epsilon_0}}$ , with  $I$  being the laser field intensity,  $c$  the speed of light, and  $\epsilon_0$  the vacuum electric permittivity. The laser intensity is fixed to  $I = 5 \times 10^{11} \text{ W/cm}^2$ , and the electric-field strength is  $E_0 \approx 1.94 \times 10^7 \text{ V/cm}$ . This intensity is routinely used in nonresonant ac laser pulses, whereas it is larger than the experimentally available intensities for cw lasers [51]. The two-color field period is fixed to  $T = \frac{2\pi}{\omega} = 400 \text{ fs}$ , which is two orders of magnitude larger than the period of the nonresonant lasers used typically in experiments involving, e.g., the YAG laser and Ti:sapphire [52]. The electric-field frequencies are  $\omega$  and  $2\omega$ , i.e.,  $q_1 = 1$  and  $q_2 = 2$ , which provoke both the orientation and alignment of the molecule. Due to the phase-shift symmetry (18) of the  $t_0$ -averaged expectation values, the first-harmonic phase is fixed to zero  $\delta_1 = 0$ .

#### A. Orientation induced by the two-color laser field

In this section, the rotational dynamics of the ground state, i.e.,  $\psi(\Omega, t = 0) = Y_{0,0}(\Omega)$ , is explored in terms of the molecular orientation by systematically including in the description the interactions of the electric field with the electric dipole moment, polarizability, and hyperpolarizability of the molecule.

For  $H = H_0 + H_\mu$ , the contour plots Figs. 1(a), 1(b), and 1(c) present the  $t_0$ -averaged orientation as a function of the propagation time  $t$  and the phase of the second-harmonic  $\delta_2$  for the strength parameters  $\gamma = 0.25, 0.5$ , and  $0.75$ , respectively. For a fixed time,  $\langle\langle \cos \theta \rangle\rangle$  satisfies the symmetry (23) with  $k = 1, n_1 = 0$ , and  $n_2 = 1$ , and approximately fulfills the relation  $\langle\langle \cos \theta \rangle\rangle(t, \delta_2) \approx \langle\langle \cos \theta \rangle\rangle(t, \pi - \delta_2)$ . Regardless of the values of  $\gamma$  and  $t$ ,  $\langle\langle \cos \theta \rangle\rangle$  shows the same dependence on  $\delta_2$ , and  $|\langle\langle \cos \theta \rangle\rangle|$  reaches its maximal value for  $\delta_2 \approx \pi/2$  and  $3\pi/2$ , and the minimal one for  $\delta_2 \approx 0$  and  $\pi$ . For given  $\gamma$  and  $\delta_2$ ,  $\langle\langle \cos \theta \rangle\rangle$  oscillates as a function of time, and the field-dressed wave function has contributions of only a few field-free states. The amplitude of these oscillations is very small for  $\delta_2 \approx 0$  and  $\pi$ .

By adding the interaction of the electric field with the molecular polarizability, i.e.,  $H = H_0 + H_\mu + H_\alpha$ , the field-dressed dynamics becomes more complex. The corresponding  $t_0$ -averaged orientation is presented in Figs. 1(d), 1(e), and 1(f) for  $\gamma = 0.25, 0.5$ , and  $0.75$ , respectively. In this case,  $\langle\langle \cos \theta \rangle\rangle$  also satisfies the symmetry relation (23) for  $k = 1, n_1 = 0$ ,

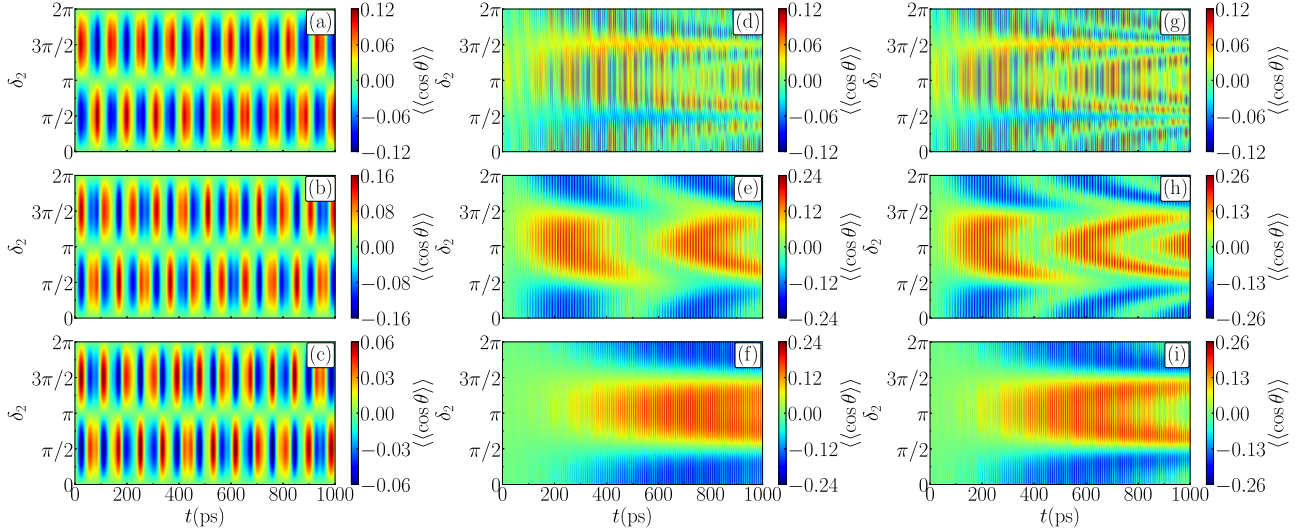


FIG. 1. Orientation averaged over  $t_0$  as a function of the time and the second-harmonic phase for the parameters (a), (d), (g)  $\gamma = 0.25$ , (b), (e), (h)  $\gamma = 0.5$ , and (c), (f), (i)  $\gamma = 0.75$ . The interaction Hamiltonian includes (a)–(c)  $H_\mu$ , (d)–(f)  $H_\mu + H_\alpha$ , and (g)–(i)  $H_\mu + H_\alpha + H_\beta$ .

and  $n_2 = 1$ . In addition, the dependence of  $\langle\langle \cos \theta \rangle\rangle$  on the second-harmonic phase for fixed time  $t$  strongly depends on the parameter  $\gamma$ , i.e., on the relative weight of the electric-field components. For  $\gamma = 0.25$ , the  $t_0$ -averaged orientation is composed of slow oscillations with superimposed fast modulations of the amplitude, and it is lower than 0.12. In contrast, an orientation up to 0.24 is achieved for  $\gamma = 0.5$  and 0.75, and  $\langle\langle \cos \theta \rangle\rangle$  slowly oscillates with time, whereas the amplitude also shows small oscillations.

The  $t_0$ -averaged orientation when the three interactions are considered,  $H = H_0 + H_\mu + H_\alpha + H_\beta$ , is presented in Figs. 1(g), 1(h), and 1(i) for  $\gamma = 0.25$ , 0.5, and 0.75, respectively. The rotational dynamics shows a qualitatively similar behavior as when  $H_\beta$  is neglected [compare panels (d)–(g), (e)–(h), and (f)–(i)]. The maximal value of the orientation is slightly larger in this case, and for fixed  $\delta_2$  the oscillations as a function of  $t$  have smaller periods.

For a fixed configuration of the two-color laser field and a certain propagation time  $t$ ,  $\langle\langle \cos \theta \rangle\rangle$  is given by the analytic expression (B8), which is illustrated in Fig. 2. Panels (a) and (b) in Fig. 2 show the  $t_0$ -averaged orientation as a function of  $\delta_2$  for propagation times  $t = 200$  and 600 ps, respectively, and the two components of the electric field having the same weight  $\gamma = 0.5$ . These curves have been numerically fitted to the expansion (B8) using the  $\delta_2$ -independent constants  $\mathcal{C}_j(t, \epsilon_1, \epsilon_2)$  and  $\varphi_j(t, \epsilon_1, \epsilon_2)$  as fitting parameters with  $j$  being an odd integer. Figures 2(c) and 2(d) show these fitted coefficients  $\mathcal{C}_j(t, \epsilon_1, \epsilon_2)$  at  $t = 200$  and 600 ps, respectively; the fitted phases are presented in Figs. 2(e) and 2(f). If only the interaction with the electric dipole moment is included, the first coefficient  $j = 1$  is sufficient to reproduce the dependence of  $\langle\langle \cos \theta \rangle\rangle$  on  $\delta_2$  with a fairly good accuracy, and the phase of this  $j = 1$  coefficient is close to  $\pi/2$ , in agreement with the observed sinelike behavior  $\langle\langle \cos \theta \rangle\rangle(t, \delta_2) \approx \langle\langle \cos \theta \rangle\rangle(t, \pi - \delta_2)$ . The next term in the expansion (B8) with  $j = 3$  is smaller than  $5 \times 10^{-5}$  for these two propagation times. The deviation of the phases  $\varphi_1(t, \epsilon_1, \epsilon_2)$  and  $\varphi_3(t, \epsilon_1, \epsilon_2)$  from being exactly  $\pi/2$  prevents the  $t_0$ -averaged orientation from being exactly

zero at  $\delta_2 = 0$  and  $\pi$ . By adding the interaction with the molecular polarizability, higher-order terms become more important in Eq. (B8). However, the  $j \geq 7$  ( $j \geq 11$ ) coefficients are smaller than  $10^{-4}$  for  $t = 200$  ps ( $t = 600$  ps). Finally, for  $H = H_0 + H_\mu + H_\alpha + H_\beta$ , the dependence of  $\langle\langle \cos \theta \rangle\rangle$  on  $\delta_2$  gets more complicated, and the contribution of higher-order terms increases, gaining importance in the expansion (B8). In these two cases, the fitted phases take values very close to  $\pi$  or  $2\pi$  [see Figs. 2(e) and 2(f)], and again the deviation from these values prevents  $\langle\langle \cos \theta \rangle\rangle$  from being zero at  $\delta_2 = \pi/2$  and  $3\pi/2$ .

This analysis is completed by investigating the dependence of the  $t_0$ -averaged orientation on the relative weight of the two electric-field components  $\gamma$  in Fig. 3. When only the interaction with the electric dipole moment is taken into account, the results for  $\delta_2 = 0, \pi/2$ , and  $3\pi/4$  are presented in Figs. 3(a), 3(b), and 3(c), respectively. As discussed in Sec. II, the  $t_0$ -averaged orientation is zero for  $\gamma = 0$  and 1 because the electric field (1) becomes one-color. For fixed  $\gamma$  and  $\delta_2$ ,  $\langle\langle \cos \theta \rangle\rangle$  shows fast oscillation versus  $t$ . The dependence of  $\langle\langle \cos \theta \rangle\rangle$  on  $\gamma$  changes as the propagation time  $t$  increases. The orientation tends to reach larger values for  $0.25 \lesssim \gamma \lesssim 0.75$ . The maximal orientation is 0.16, which is achieved for  $\delta_2 = \pi/2$ . The orientation for  $\delta_2 = 0$  is nonzero but lower than  $10^{-3}$ .

For  $H = H_0 + H_\mu + H_\alpha$ , Figs. 3(d), 3(e), and 3(f) present  $\langle\langle \cos \theta \rangle\rangle$  for  $\delta_2 = 0, \pi/2$ , and  $3\pi/4$ , respectively. Compared to the previous case, the dependence of  $\langle\langle \cos \theta \rangle\rangle$  on  $\gamma$  and  $t$  has notably changed. As a function of  $t$ ,  $\langle\langle \cos \theta \rangle\rangle$  shows slow oscillations, the amplitude of which is modulated. A moderate orientation of the molecule is attained for several values of  $\gamma$ . The maximal absolute value of the orientation is reached for  $\delta_2 = 0, \pi$  (not shown here), and  $3\pi/4$ , whereas the minimal one occurs for  $\delta_2 = \pi/2$ , when  $|\langle\langle \cos \theta \rangle\rangle|$  is smaller than 0.08. By adding the interaction with the hyperpolarizability, i.e.,  $H = H_0 + H_\mu + H_\alpha + H_\beta$ ,  $\langle\langle \cos \theta \rangle\rangle$  is not significantly modified, and possesses a qualitatively similar dependence on  $t$  and  $\gamma$  as in the previous case [see Figs. 3(g), 3(h), and 3(i)].



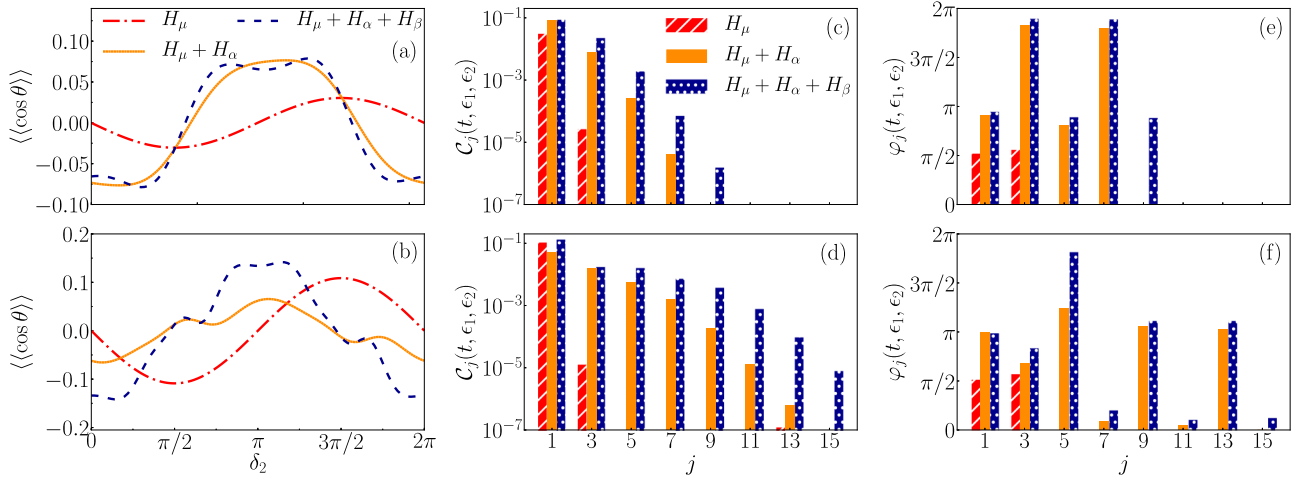


FIG. 2. For a two-color electric field with  $\gamma = 0.5$ ,  $t_0$ -averaged orientation as a function of the second-harmonic phase at fixed propagation times (a)  $t = 200$  ps and (b)  $t = 600$  ps. (c), (d) Fitted coefficients  $C_j(t, \epsilon_1, \epsilon_2)$  and (e), (f) fitted phases  $\varphi_j(t, \epsilon_1, \epsilon_2)$  from the analytic expression (B8) of  $\langle\langle \cos \theta \rangle\rangle$  for  $t = 200$  and 600 ps, respectively. The interaction Hamiltonian includes  $H_\mu$  (red dot-dashed line, histograms red dashed),  $H_\mu + H_\alpha$  (orange solid line), and  $H_\mu + H_\alpha + H_\beta$  (blue dashed line, histograms blue dotted).

### B. Alignment induced by the two-color laser field

The  $t_0$ -averaged alignment of the ground state in a two-color laser field with period  $T = 400$  fs is presented as a function of  $t$  and  $\delta_2$  in Fig. 4. For all considered configurations,  $\langle\langle \cos^2 \theta \rangle\rangle$  satisfies the symmetry relation (23) with  $k = 2$ ,  $n_1 = 0$ , and  $n_2 = 1$ . For  $H = H_0 + H_\mu$ ,  $\langle\langle \cos^2 \theta \rangle\rangle$  depends very weakly on  $\delta_2$ , and oscillates as  $t$  increases quasiperiodically between 0.3 and 0.6 [see Fig. 4(a)]. By also taking into account the interaction with the molecular polarizability and with the hyperpolarizability,  $\langle\langle \cos^2 \theta \rangle\rangle$  shows a rather weak dependence on  $\delta_2$  for short propagation times, which becomes stronger for  $t \gtrsim 200$  ps [see Figs. 4(b) and 4(c)]. In these cases, the oscillations of  $\langle\langle \cos^2 \theta \rangle\rangle$  as a function of  $t$  are faster,

and the molecule becomes strongly aligned with  $\langle\langle \cos^2 \theta \rangle\rangle$ , reaching up to 0.9.

The analytic expression (B9) provides the dependence of  $\langle\langle \cos^2 \theta \rangle\rangle$  on  $\delta_2$ . In Fig. 5(a) and 5(b),  $\langle\langle \cos^2 \theta \rangle\rangle$  is plotted as a function of the second-harmonic phase for  $\gamma = 0.5$  and propagation times  $t = 200$  and 600 ps, respectively. The numerical results have been fitted to the series (B9), and the coefficients  $C_j(t, \epsilon_1, \epsilon_2)$  and phases  $\varphi_j(t, \epsilon_1, \epsilon_2)$ , with  $j$  an even integer, are presented in Figs. 5(c)–5(d), and 5(e)–5(f), respectively. When only the electric-field interaction with the electric dipole moment is taken into account, the alignment depends very weakly on  $\delta_2$ , and  $C_0(t, \epsilon_1, \epsilon_2)$  is the only fitting parameter accurately reproducing this result. The next term

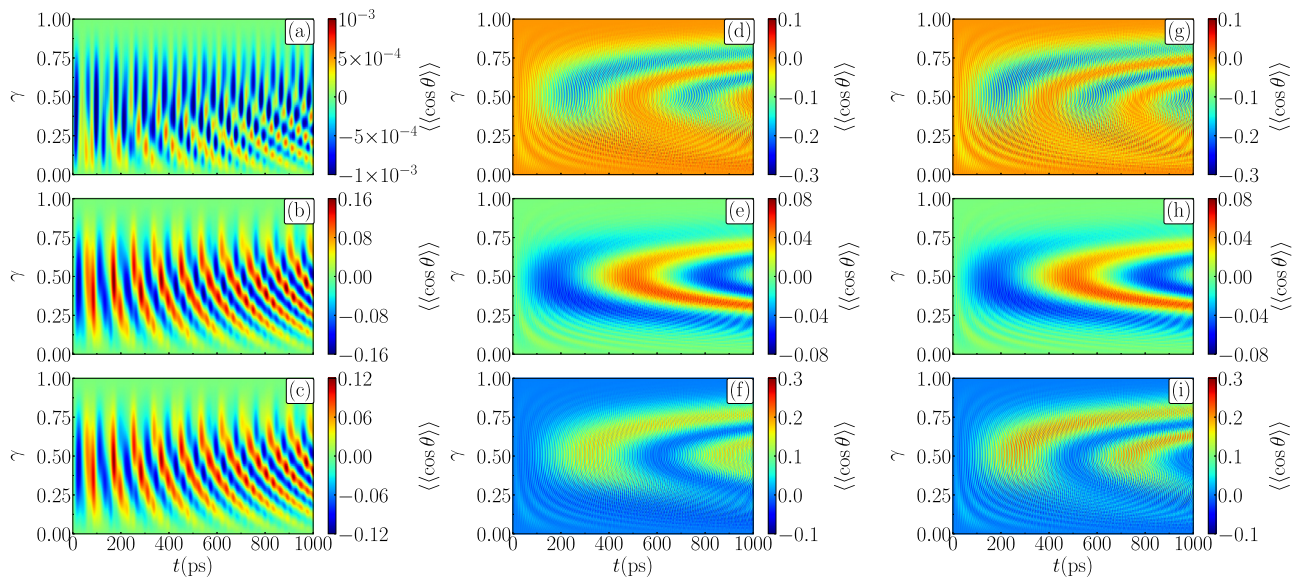


FIG. 3. The  $t_0$ -averaged orientation as a function of the propagation time and of the relative weight of the two electric-field components  $\gamma$  for the phase of the second-harmonic (a), (d), (g)  $\delta_2 = 0$ , (b), (e), (h)  $\delta_2 = \pi/2$ , and (c), (f), (i)  $\delta_2 = 3\pi/4$ . The interaction Hamiltonian includes (a)–(c)  $H_\mu$ , (d)–(f)  $H_\mu + H_\alpha$ , and (g)–(i)  $H_\mu + H_\alpha + H_\beta$ .

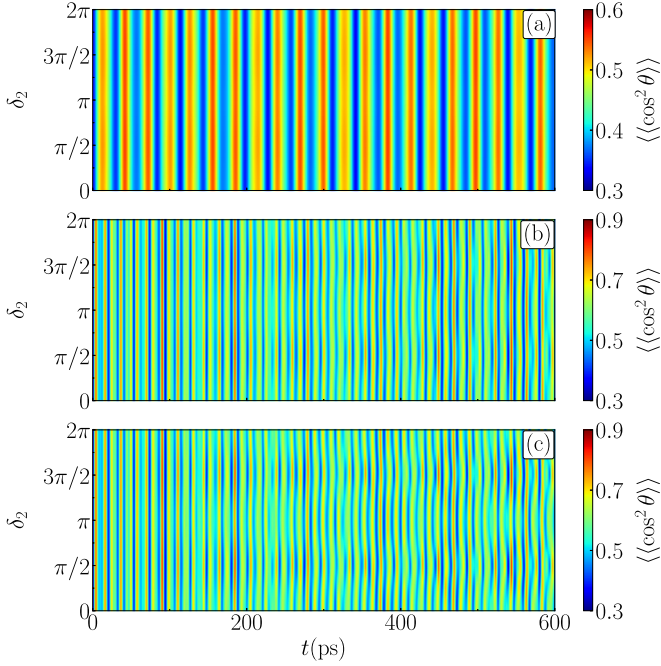


FIG. 4. The  $t_0$ -averaged alignment as a function of the propagation time and the second-harmonic phase  $\delta_2$  for the relative weight of the electric-field components  $\gamma = 0.5$ , including the interactions (a)  $H_\mu$ , (b)  $H_\mu + H_\alpha$ , and (c)  $H_\mu + H_\alpha + H_\beta$ .

$C_2(t, \epsilon_1, \epsilon_2)$  is smaller than  $2 \times 10^{-4}$ . For  $H = H_0 + H_\mu + H_\alpha$ , higher-order terms are needed in the  $\langle\langle \cos^2 \theta \rangle\rangle$  analytical expansion, and the  $j \geq 6$  and 8 coefficients become smaller than  $10^{-4}$  for  $t = 200$  and 600 ps, respectively. For  $H = H_0 + H_\mu + H_\alpha + H_\beta$ , the  $\delta_2$  dependence of  $\langle\langle \cos^2 \theta \rangle\rangle$  becomes more complex, and even higher-order terms are required for an accurate fitting. In these two cases, a broad range of values is encountered for  $\varphi_j(t, \epsilon_1, \epsilon_2)$  shown in Figs. 5(e) and 5(f).

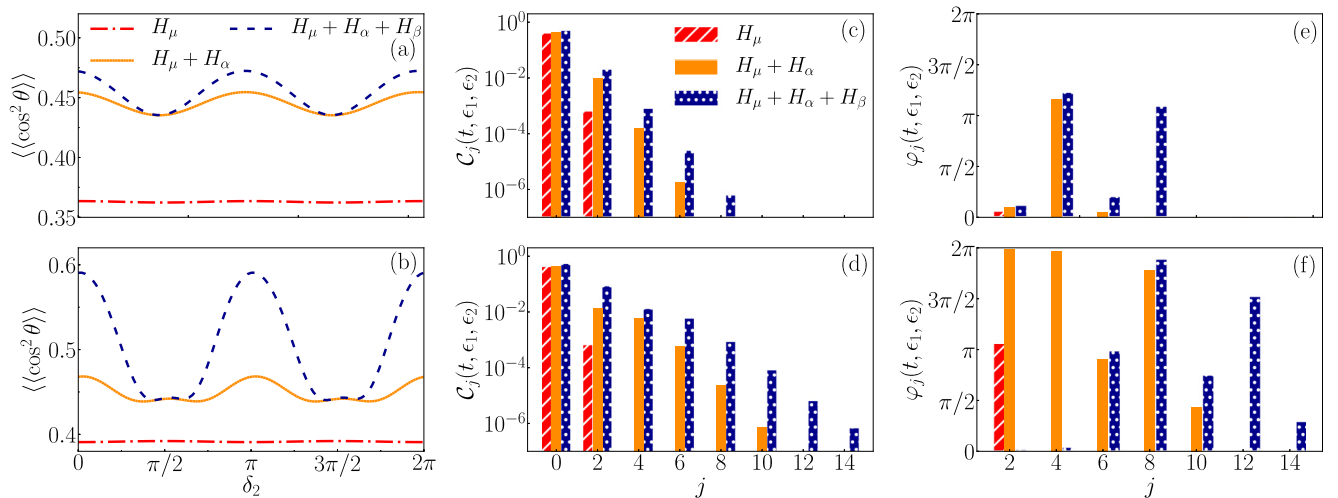


FIG. 5. For a two-color electric field with  $\gamma = 0.5$ ,  $t_0$ -averaged alignment as a function of the second-harmonic phase at fixed propagation times (a)  $t = 200$  ps and (b)  $t = 600$  ps. (c), (d) Fitted coefficients  $C_j(t, \epsilon_1, \epsilon_2)$  and (e), (f) fitted phases  $\varphi_j(t, \epsilon_1, \epsilon_2)$  from the analytic expression (B9) of  $\langle\langle \cos^2 \theta \rangle\rangle$  for  $t = 200$  and 600 ps, respectively. The interaction Hamiltonian includes  $H_\mu$  (red dot-dashed line, histograms red dashed),  $H_\mu + H_\alpha$  (orange solid line), and  $H_\mu + H_\alpha + H_\beta$  (blue dashed line, histograms blue dotted).

Figure 6 presents  $\langle\langle \cos^2 \theta \rangle\rangle$  as a function of  $\gamma$  and  $t$  for  $\delta_2 = 3\pi/4$ . If only the electric-field interaction with the electric dipole moment is considered [see Fig. 6(a)], the  $t_0$  alignment oscillates between 0.3 and 0.7, and reaches the largest values for  $\gamma < 0.5$  when the first-harmonic field is the strongest. For fixed  $\gamma$ ,  $\langle\langle \cos^2 \theta \rangle\rangle$  shows quite regular oscillations as a function of time. By taking into account the electric-field interaction with the polarizability and with both polarizability and hyperpolarizability [see Figs. 6(b) and 6(c), respectively],  $\langle\langle \cos^2 \theta \rangle\rangle$  reaches larger values, up to 0.9, and the frequency of the oscillations is increased.

### C. Rotational dynamics of a thermal sample

The field-dressed rotational dynamics of excited rotational states shows a similar dependence on the symmetries of the Hamiltonian and, therefore, on the laser field parameters. Figure 7 presents the time evolution of the  $t_0$ -averaged orientation of thermal samples with rotational temperatures  $T_{\text{rot}} = 0.5$  and 2 K, as a function of second-harmonic phase and for  $\gamma = 0.5$ . Due to the contribution of higher excited rotational states, the extreme values of the  $t_0$ -average orientation of the thermal sample  $\langle\langle \cos \theta \rangle\rangle_{\mathcal{T}}$  are significantly reduced as the temperature increases, but  $\langle\langle \cos \theta \rangle\rangle_{\mathcal{T}}$  still satisfies the symmetry Eq. (23). For  $H = H_0 + H_\mu$ ,  $\langle\langle \cos \theta \rangle\rangle_{\mathcal{T}}$  possesses a sine-like behavior as a function of  $\delta_2$ . By including the interactions due to the polarizability and hyperpolarizability, this dependence on  $\delta_2$  becomes more complex. For a fixed  $\delta_2$ , the time evolution of  $\langle\langle \cos \theta \rangle\rangle_{\mathcal{T}}$  is similar to the one of the ground state presented in Fig. 1, which is equivalent to a  $T_{\text{rot}} = 0$  K thermal sample.

The analytic expression (B8) is used to explore the orientation of these thermal samples. For  $t = 600$  ps, the fitted coefficients  $C_j(t, \epsilon_1, \epsilon_2)$  and phases  $\varphi_j(t, \epsilon_1, \epsilon_2)$ , with  $j$  an odd integer, are presented in Fig. 8. For both temperatures, the coefficients possess similar values, whereas more differences

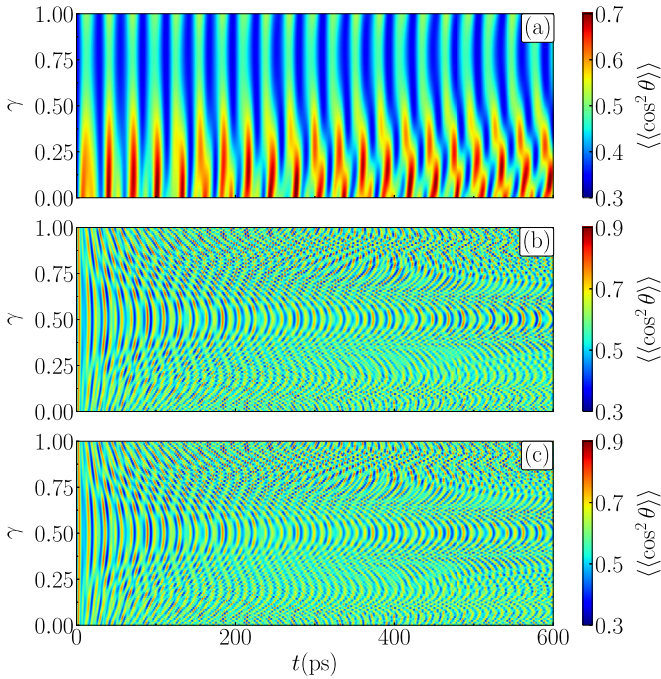


FIG. 6. The  $t_0$ -averaged alignment as a function of the propagation time and the relative weight of the electric-field components  $\gamma$  for the second-harmonic phase  $\delta_2 = 3\pi/4$ , including the interactions (a)  $H_\mu$ , (b)  $H_\mu + H_\alpha$ , and (c)  $H_\mu + H_\alpha + H_\beta$ .

are encountered on the phases. As for the ground state, the coefficients with higher values of  $j$  increase as the interactions are progressively included in the description.

The  $t_0$ -averaged alignment of a thermal sample with rotational temperature  $T_{\text{rot}} = 2$  K is plotted in Fig. 9. For short propagation times,  $\langle\langle \cos^2 \theta \rangle\rangle_{\mathcal{T}}$  possesses a constant behavior as a function of  $\delta_2$ . This behavior is also observed for larger times when only the interaction with the electric dipole moment is taken into account. For larger times,  $\langle\langle \cos^2 \theta \rangle\rangle_{\mathcal{T}}$  presents oscillations as a function of  $\delta_2$  with a rather small amplitude. Overall, the alignment is significantly reduced due to the contribution of higher excited states.

#### IV. CONCLUSIONS

The implications of the symmetries in the field-dressed rotational dynamics of a linear polar molecule in a two-color continuous-wave nonresonant laser field have been discussed and analyzed in detail. The system has been investigated in the framework of the rigid-rotor approximation and in a regime where the time-average approximation is not correct. For the expectation values  $\langle \cos^k \theta \rangle$  and  $\langle\langle \cos^k \theta \rangle\rangle$ , a collection of identities is derived based on the Hamiltonian symmetries. These identities are satisfied independently of the initial state, i.e., they also hold for a thermal sample, and of the dipole-expansion terms of the interaction due to the two-color cw laser field included in the Hamiltonian. By systematically considering the interactions of this field with the electric dipole moment, polarizability, and hyperpolarizability, the field-dressed rotational dynamics becomes gradually more complex. In particular, this paper shows that the interaction of a two-color cw laser field with the electric dipole moment cannot be neglected as is done for two-color laser pulses. Furthermore, the small differences encountered in the dynamics by including or neglecting the hyperpolarizability interaction indicate that interactions due to higher hyperpolarizability terms might be negligible.

Due to these symmetries, the orientation and alignment can be expressed as analytic functions of the phases and strengths of the two components of the two-color cw laser field. The numerical analysis demonstrates that only a few terms have a significant contribution on the expansion series, and their weights increase as the interactions with the electric dipole moment, polarizability, and hyperpolarizability are taken into account. The effect of symmetries of the two-color electric field on the orientation and alignment is very different, and depends on the interactions included in the description. In addition, it is analytically shown that a one-color cw laser field does not orient the molecule. To orient the molecule a cw two-color laser having odd and even multiples of the laser frequency is required. The largest orientation and alignment are not necessarily obtained when the two components of the two-color cw laser field have the same weight. Furthermore, the rotational dynamics can be computed for fixed values of the phases,  $\delta_1$  and  $\delta_2$ , and is the same for any phases satisfying  $\tilde{\delta}_1 = \delta_1 + q_1 \Delta$  and  $\tilde{\delta}_2 = \delta_2 + q_2 \Delta$ . The time-reversal

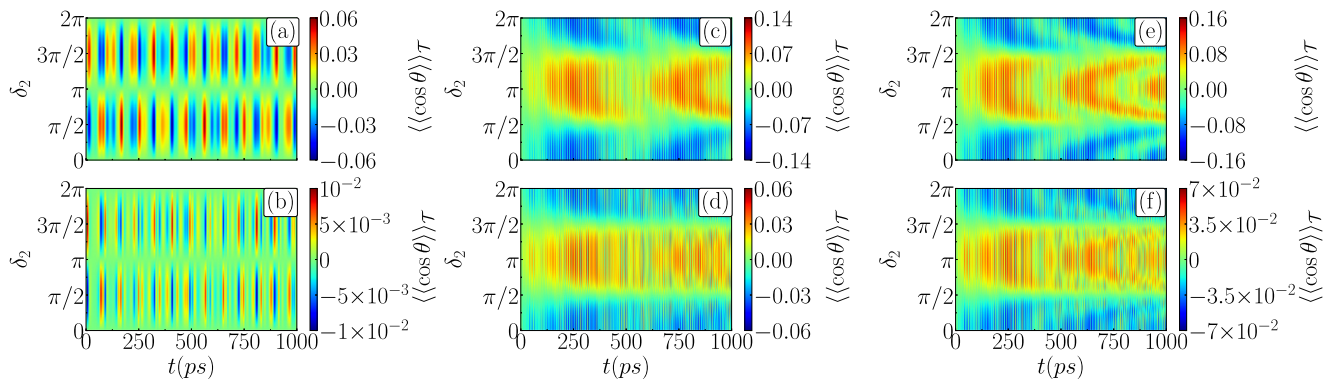


FIG. 7. For a thermal sample,  $t_0$ -averaged orientation as a function of the propagation time and the second-harmonic phase for  $\gamma = 0.5$ , including the interactions (a), (b)  $H_\mu$ , (c), (d)  $H_\mu + H_\alpha$ , and (e), (f)  $H_\mu + H_\alpha + H_\beta$  and rotational temperatures  $T_{\text{rot}} = 0.5$  and 2 K, respectively.



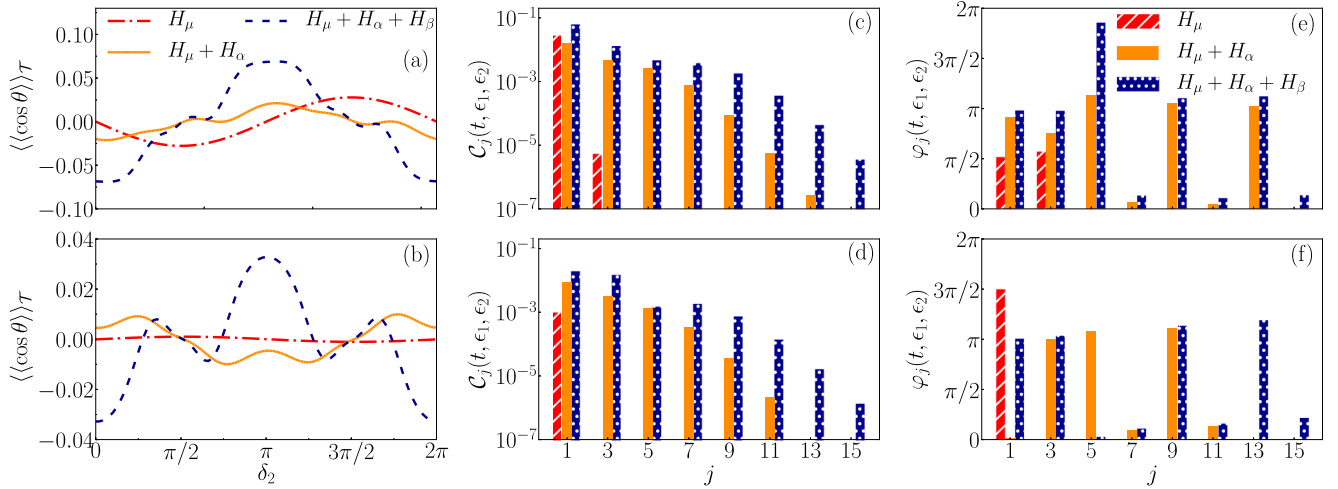


FIG. 8. For a thermal sample, (a), (b)  $t_0$ -averaged orientation as a function of the second-harmonic phase at fixed propagation time  $t = 600$  ps, (c), (d) fitted coefficients  $C_j(t, \epsilon_1, \epsilon_2)$ , and (e), (f) fitted phases  $\varphi_j(t, \epsilon_1, \epsilon_2)$  from the analytic expression (B8) of  $\langle\langle \cos \theta \rangle\rangle$  for rotational temperatures  $T_{\text{rot}} = 0.5$  and 2 K, respectively. The interaction Hamiltonian includes  $H_\mu$  (red dot-dashed line, histograms red dashed),  $H_\mu + H_\alpha$  (orange solid line), and  $H_\mu + H_\alpha + H_\beta$  (blue dashed line, histograms blue dotted).

symmetry is also satisfied for certain parameters of the applied field. Finally, the validity of the time-average approximation has been also investigated assuming that this cw nonresonant field does not drive any electronic, vibrational, or rotational transitions.

Although this paper is restricted to the OCS molecule, the observed physical phenomena occur for any linear polar molecule. For each specific linear molecule, a detailed numerical analysis is required to determine the importance of

the three interactions in the field-dressed Hamiltonian, and their impact in the rotational dynamics. A natural extension to this paper would be to consider a linear polar molecule in a two-color cw laser field with the two components having perpendicular polarizations [54]. In this field configuration, the symmetries of the system are reduced, and the two field components tend to align and orient the molecule in different directions. In addition, more complex molecules, such as symmetric or asymmetric tops, in a two-color cw nonresonant laser field could be also explored.

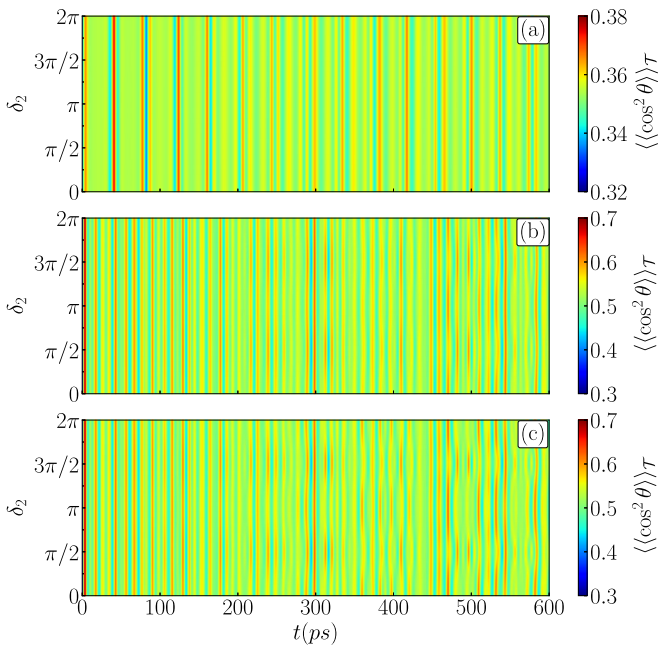


FIG. 9. For a thermal sample with rotational temperature  $T_{\text{rot}} = 2$  K, the  $t_0$ -averaged alignment as a function of the time and the second-harmonic phase for  $\gamma = 0.5$ , including the interactions (a)  $H_\mu$ , (b)  $H_\mu + H_\alpha$ , and (c)  $H_\mu + H_\alpha + H_\beta$ .

## ACKNOWLEDGMENTS

N.R.Q. acknowledges financial support from the Alexander von Humboldt Foundation. Financial support by the Spanish MINECO Project No. FIS2017-89349-P, and by the Andalusian research group FQM-207, is gratefully acknowledged. This study has been partially financed by the Consejería de Conocimiento, Investigación y Universidad, Junta de Andalucía, and European Regional Development Fund, Grant No. SOMM17/6105/UGR. R.G.F. completed some of this work as a Fulbright fellow at ITAMP at Harvard University.

## APPENDIX A: VALIDITY OF THE TIME-AVERAGE APPROXIMATION

This section is devoted to investigate the validity of the time-average approximation [47]. For a nonresonant two-color laser field, if the field frequencies,  $\omega$  and  $2\omega$ , are far from any molecular resonance and higher than the molecular rotational frequency, the Hamiltonian (2) is averaged over the rapid oscillations of the nonresonant laser field. Note that for a laser pulse, it is further assumed that the laser period is much shorter than the pulse duration. If the time-average approximation is correct, then the Hamiltonian (2) is



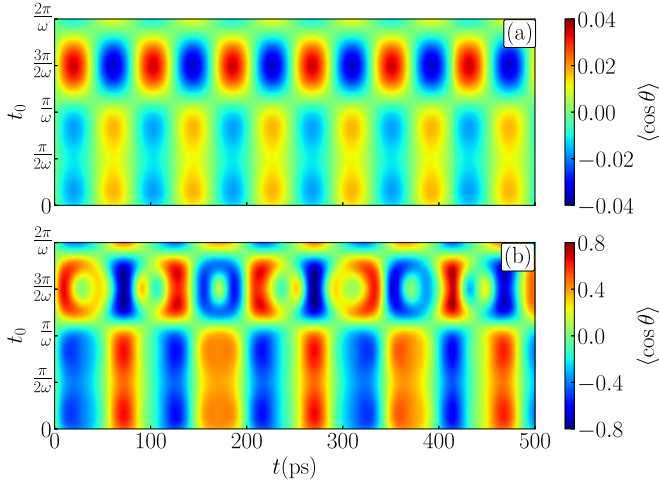


FIG. 10. For the ground state  $\psi(\Omega, t = 0) = Y_{0,0}(\Omega)$  and  $H = H_0 + H_\mu$ , orientation as a function of time and  $t_0$  for a two-color laser field with periods (a)  $T = 10$  fs and (b)  $T = 400$  fs, and  $\gamma = 0.5$ ,  $\delta_1 = 0$ , and  $\delta_2 = \pi/2$ .

reduced to

$$H = B\mathbf{J}^2 - \frac{1}{2}\Delta\alpha \cos^2\theta f_1(\epsilon_1, \epsilon_2, q_1, q_2, \delta_1, \delta_2) - \frac{1}{6}(\Delta\beta \cos^3\theta + 3\beta_\perp \cos\theta) f_2(\epsilon_1, \epsilon_2, q_1, q_2, \delta_1, \delta_2) \quad (\text{A1})$$

with

$$f_1(\epsilon_1, \epsilon_2, q_1, q_2, \delta_1, \delta_2) = \frac{\epsilon_1^2 + \epsilon_2^2}{2} + \epsilon_1\epsilon_2 \cos(\delta_1 - \delta_2)\delta_{q_1, q_2},$$

$$f_2(\epsilon_1, \epsilon_2, q_1, q_2, \delta_1, \delta_2) = \frac{3}{4}\epsilon_1^2\epsilon_2\delta_{2q_1, q_2} \cos(2\delta_1 - \delta_2) + \frac{3}{4}\epsilon_1\epsilon_2^2\delta_{q_1, 2q_2} \cos(\delta_1 - 2\delta_2).$$

For a two-color electric field with  $q_1 = 1$  and  $q_2 = 2$ , the time-averaged Hamiltonian (A1) reads

$$H = B\mathbf{J}^2 - \frac{1}{4}\Delta\alpha \cos^2\theta(\epsilon_1^2 + \epsilon_2^2) - \frac{1}{8}(\Delta\beta \cos^3\theta + 3\beta_\perp \cos\theta)\epsilon_1^2\epsilon_2 \cos(2\delta_1 - \delta_2). \quad (\text{A2})$$

Thus, depending on the values of the phases  $\delta_1$  and  $\delta_2$ , this time-averaged Hamiltonian might align the molecule, or both orient and align it.

In particular, a one-color laser field should not orient the molecules. Considering only the interaction with the electric dipole moment and  $\epsilon_2 = 0$ ,  $|\langle \cos\theta \rangle| \gtrsim 10^{-2}$  for  $T \gtrsim 10$  fs and  $|\langle \langle \cos\theta \rangle \rangle| \approx 10^{-8}$ , whereas for  $T = 1$  fs,  $|\langle \cos\theta \rangle| \approx 10^{-3}$  and  $|\langle \langle \cos\theta \rangle \rangle| \approx 10^{-9}$ . In the regime  $T \gtrsim 10$  fs the time-average approximation starts to fail. For  $T = 10$  fs, the maximal deviations of the alignment from its field-free value are  $|\langle \cos^2\theta \rangle - 1/3| \lesssim 10^{-3}$  and  $|\langle \langle \cos^2\theta \rangle \rangle - 1/3| \lesssim 10^{-4}$ . For  $H = H_0 + H_\mu + H_\alpha + H_\beta$  and  $T \gtrsim 10$  fs,  $|\langle \cos\theta \rangle| \gtrsim 10^{-2}$ , whereas  $\langle \cos^2\theta \rangle$  and  $\langle \langle \cos^2\theta \rangle \rangle$  each take values up to 0.85.

For a two-color laser field and  $H = H_0 + H_\mu$ , Figs. 10(a) and 10(b) show the orientation as a function of  $t$  and  $t_0$  for laser field periods 10 and 400 fs, respectively, and the field parameters  $\gamma = 0.5$  and  $\delta_2 = \pi/2$ . The orientation is nonzero

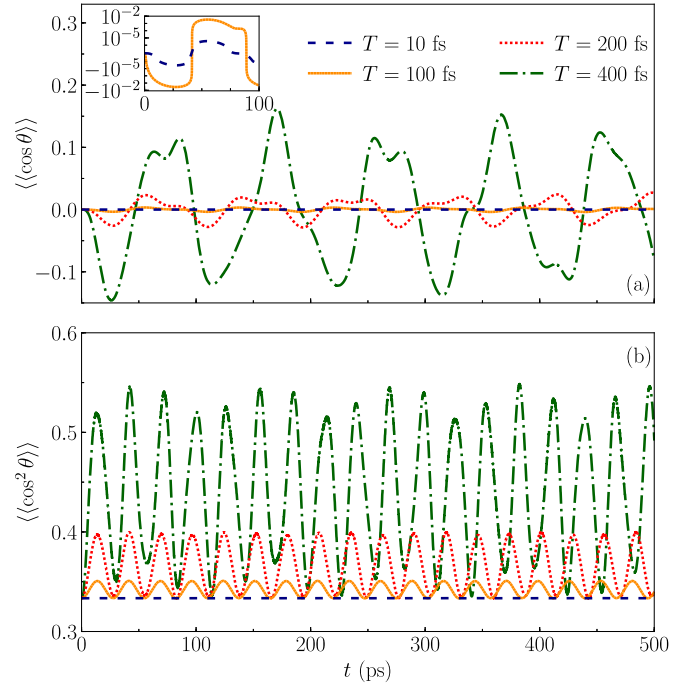


FIG. 11. For the ground state  $\psi(\Omega, t = 0) = Y_{0,0}(\Omega)$  and the Hamiltonian  $H = H_0 + H_\mu$ , (a) orientation and (b) alignment averaged over  $t_0$  as a function of time for the electric-field periods  $T = 10$  fs (blue dashed line), 100 fs (orange solid line), 200 fs (red dotted line), and 400 fs (green dot-dashed line). The electric-field parameters are fixed to  $\gamma = 0.5$ ,  $\delta_1 = 0$ , and  $\delta_2 = \pi/2$ .

even for  $T = 10$  fs, and depends on  $t_0$ . These two features contradict the validity of the time-average approximation. Figure 11 presents the  $t_0$ -averaged orientation and  $t_0$ -averaged alignment as a function of  $t$  for  $T = 10, 100, 200$ , and 400 fs, and  $\gamma = 0.5$  and  $\delta_2 = \pi/2$ . For  $T = 10$  fs, the  $t_0$ -averaged orientation is of the order of  $10^{-6}$ . Note that  $|\langle \cos\theta \rangle|$  is four orders of magnitude larger, but due to the dependence of  $\langle \cos\theta \rangle$  on  $t_0$  [see Fig. 10(a)]  $\langle \langle \cos\theta \rangle \rangle$  becomes very small. The maximal deviation of the  $t_0$ -averaged alignment from its field-free value is  $1.8 \times 10^{-4}$ . Thus, for  $T = 10$  fs, on average the molecule is neither oriented nor aligned. One could conclude that the time-average approximation can be applied; however, for a fixed  $t_0$ , it is not correct as shown in Fig. 10(a). For  $T = 100$  fs, the deviations of  $\langle \langle \cos\theta \rangle \rangle$  and  $\langle \langle \cos^2\theta \rangle \rangle$  from the corresponding field-free values are still small but not negligible. By increasing  $T$ , i.e., reducing the laser frequency  $\omega$ ,  $\langle \langle \cos\theta \rangle \rangle$  and  $\langle \langle \cos^2\theta \rangle \rangle$  increase; see, for instance, the results for  $T = 200$  and 400 fs.

For  $H = H_0 + H_\mu + H_\alpha + H_\beta$ , Figs. 12(a) and 12(b) show the orientation as a function of  $t_0$  and time for the laser field periods  $T = 10$  and 400 fs, respectively, and the electric-field parameters  $\gamma = 0.5$  and  $\delta_2 = \pi/2$ . As in the previous case,  $\langle \cos\theta \rangle$  is nonzero and depends on  $t_0$ , which indicates that even for a  $T = 10$  fs laser the time-average approximation is not correct. Figure 13 shows  $\langle \langle \cos\theta \rangle \rangle$  and  $\langle \langle \cos^2\theta \rangle \rangle$  as a function of  $t$  for the electric-field periods  $T = 10, 100, 200$ , and 400 fs. Due to the dependence on  $t_0$  of  $\langle \cos\theta \rangle$ , the  $t_0$ -averaged orientation is rather small even for the laser period 400 fs. This cancellation does not occur for  $\langle \langle \cos^2\theta \rangle \rangle$  because

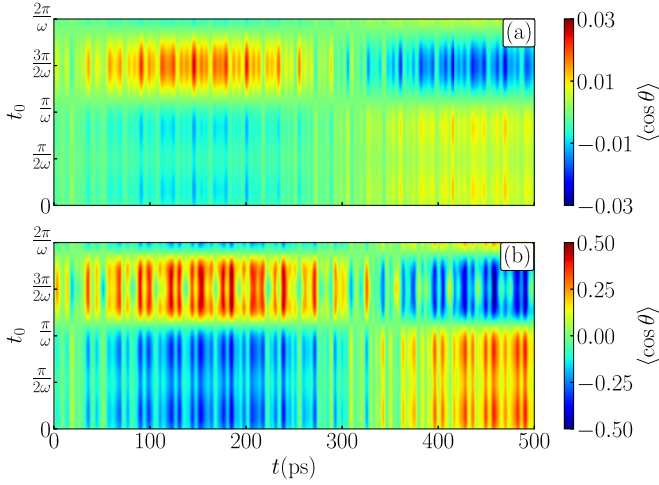


FIG. 12. For the ground state  $\psi(\Omega, t = 0) = Y_{0,0}(\Omega)$  and  $H = H_0 + H_\mu + H_\alpha + H_\beta$ , orientation as a function of time and  $t_0$  for a two-color laser field with periods (a)  $T = 10$  fs and (b)  $T = 400$  fs, and  $\gamma = 0.5$ ,  $\delta_1 = 0$ , and  $\delta_2 = \pi/2$ .

$\langle \cos^2 \theta \rangle > 0$ , and  $\langle \langle \cos^2 \theta \rangle \rangle$  is very large for all considered laser field periods.

We have obtained similar results for excited rotational states. For the initial state  $\psi(\Omega, t = 0) = Y_{2,2}(\Omega)$ ,  $\langle \langle \cos \theta \rangle \rangle$  and  $\langle \langle \cos^2 \theta \rangle \rangle$  are presented as a function of time in Figs. 14(a) and 14(b), respectively, for the electric-field periods  $T = 10$ , 100, 200, and 400 fs. Due to its large rotational kinetic energy,

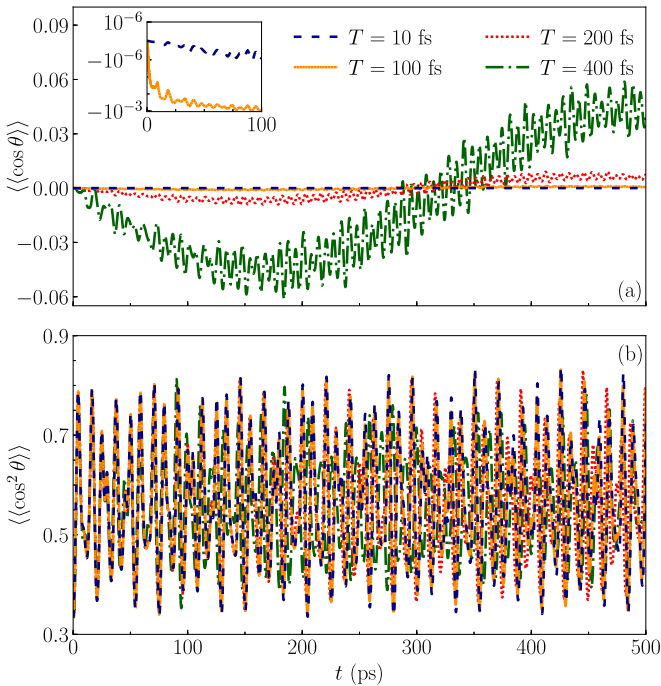


FIG. 13. For the ground state  $\psi(\Omega, t = 0) = Y_{0,0}(\Omega)$  and the three interactions, (a) orientation and (b) alignment averaged over  $t_0$  as a function of time for the electric-field periods  $T = 2\pi/\omega = 10$  fs (blue dashed line), 100 fs (orange solid line), 200 fs (red dotted line), and 400 fs (green dot-dashed line). The two-color electric-field parameters are fixed to  $\gamma = 0.5$ ,  $\delta_1 = 0$ , and  $\delta_2 = \pi/2$ .

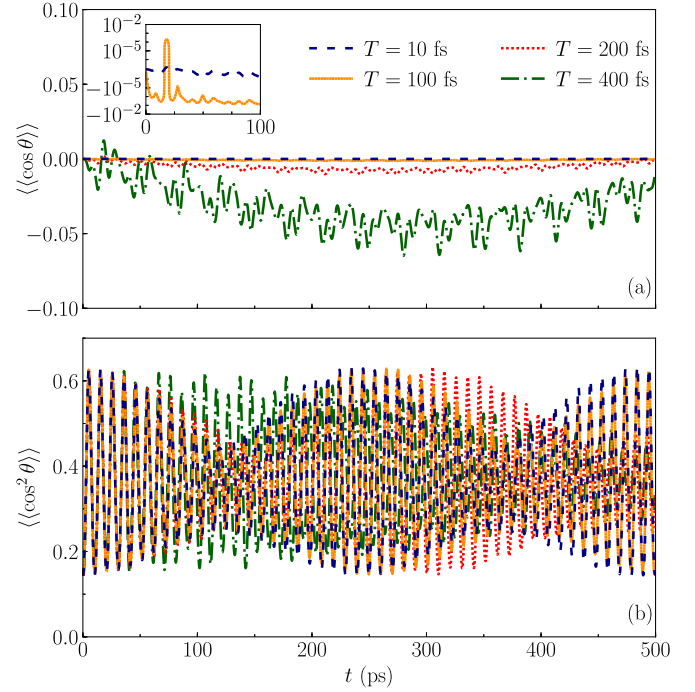


FIG. 14. For the excited state  $\psi(\Omega, t = 0) = Y_{2,2}(\Omega)$  and including the three interactions,  $t_0$ -averaged (a) orientation and (b) alignment as a function of time for the electric-field periods  $T = 2\pi/\omega = 10$  fs (blue dashed line), 100 fs (orange solid line), 200 fs (red dotted line), and 400 fs (green dot-dashed line). The two-color electric-field parameters are fixed to  $\gamma = 0.5$ ,  $\delta_1 = 0$ , and  $\delta_2 = \pi/2$ .

this excited state is less aligned than the ground state for  $T = 400$  fs, and weakly oriented. At this laser period, the deviations from the time-average approximation are the largest.

## APPENDIX B: ANALYTIC EXPRESSIONS OF THE ORIENTATION AND ALIGNMENT

Following the results of Refs. [17–19], the orientation and the alignment can be expressed in terms of the amplitude and phase,  $\epsilon_j$  and  $\delta_j$ , of the  $j$  harmonics  $g_j(t, t_0, \epsilon_j, \delta_j) = \epsilon_j \cos[q_j \omega(t + t_0) + \delta_j]$ , with  $j = 1, \dots, s$ , appearing in the Hamiltonian (2) due to the interaction of the molecule with the two-color electric field (1). The frequencies, amplitudes, and phases of these harmonics are collected in Table II. The first two rows in Table II with  $j = 1$  and 2 provide the harmonics of the biharmonic field, which appear due to the interaction of this field with the permanent electric dipole moment. The interaction of the biharmonic electric field with the polarizability is proportional to  $E^2(t)$ , and the harmonics with  $j = 3, \dots, 6$  (see Table II) also contribute to the Hamiltonian. The cubic term  $E^3(t)$  is due to interaction with the molecular hyperpolarizability, and is responsible for the harmonics with  $7 \leq j \leq 14$  in Table II.

Based on simple symmetry considerations of the  $s$  harmonic functions (see Refs. [18,19]), the orientation and the

TABLE II. Prefactor of the frequency  $\omega$ ,  $q_j$ ; amplitude,  $\epsilon_j$ ; and phase,  $\delta_j$ , of the  $j$ -harmonics appearing in the Hamiltonian (2) due to the interaction with the two-color electric field (1).

$j$	$q_j$	$\epsilon_j$	$\delta_j$
1	$q_1$	$\epsilon_1$	$\delta_1$
2	$q_2$	$\epsilon_2$	$\delta_2$
3	$2q_1$	$\epsilon_1^2/2$	$2\delta_1$
4	$2q_2$	$\epsilon_2^2/2$	$2\delta_2$
5	$q_1 + q_2$	$\epsilon_1\epsilon_2$	$\delta_1 + \delta_2$
6	$q_2 - q_1$	$\epsilon_1\epsilon_2$	$\delta_2 - \delta_1$
7	$q_1$	$(3/2)\epsilon_1\epsilon_2^2 + (3/4)\epsilon_1^3$	$\delta_1$
8	$q_2$	$(3/2)\epsilon_1^2\epsilon_2 + (3/4)\epsilon_2^3$	$\delta_2$
9	$3q_1$	$\epsilon_1^3/4$	$3\delta_1$
10	$3q_2$	$\epsilon_2^3/4$	$3\delta_2$
11	$q_2 + 2q_1$	$(3/4)\epsilon_1^2\epsilon_2$	$\delta_2 + 2\delta_1$
12	$q_2 - 2q_1$	$(3/4)\epsilon_1^2\epsilon_2$	$\delta_2 - 2\delta_1$
13	$2q_2 + q_1$	$(3/4)\epsilon_1\epsilon_2^2$	$2\delta_2 + \delta_1$
14	$2q_2 - q_1$	$(3/4)\epsilon_1\epsilon_2^2$	$2\delta_2 - \delta_1$

alignment can be expressed as

$$\begin{aligned} & \langle \cos^k \theta \rangle(t, t_0, \boldsymbol{\epsilon}, \boldsymbol{\delta}) \\ &= \sum_{\mathbf{n} \in \mathbb{Z}^s} C_n(t, \boldsymbol{\epsilon}) \prod_{j=1}^s \epsilon_j^{|\mathbf{n}_j|} \cos[\mathbf{n} \cdot \boldsymbol{\delta} + \omega t_0 \mathbf{n} \cdot \mathbf{q} + \Theta_n(t, \boldsymbol{\epsilon})], \end{aligned} \quad (\text{B1})$$

where  $\mathbf{q} = \{q_1, \dots, q_s\}$ ,  $\boldsymbol{\epsilon} = \{\epsilon_1, \dots, \epsilon_s\}$ ,  $\boldsymbol{\delta} = \{\delta_1, \dots, \delta_s\}$ , and  $C_n(t, \boldsymbol{\epsilon})$  and  $\Theta_n(t, \boldsymbol{\epsilon})$  are both even functions of each  $\epsilon_j$ . The  $t_0$ -averaged expectation value satisfies [19]

$$\begin{aligned} & \langle \langle \cos^k \theta \rangle \rangle(t, \boldsymbol{\epsilon}, \boldsymbol{\delta}) \\ &= C_0(t, \boldsymbol{\epsilon}) + \sum_{\mathbf{n} \in \mathbb{S}} C_n(t, \boldsymbol{\epsilon}) \prod_{j=1}^s \epsilon_j^{|\mathbf{n}_j|} \cos[\mathbf{n} \cdot \boldsymbol{\delta} + \Theta_n(t, \boldsymbol{\epsilon})], \end{aligned} \quad (\text{B2})$$

where

$$\mathbb{S} = \{\mathbf{n} \in \mathbb{Z}^s : \mathbf{n} \cdot \mathbf{q} = 0\} \quad (\text{B3})$$

denotes the set of nonzero solutions of the Diophantine equation  $\mathbf{n} \cdot \mathbf{q} = 0$ , the leftmost nonzero component of which is positive [18].

For  $H = H_0 + H_\mu$ ,  $s = 2$ , and  $\mathbf{q} = \{q_1, q_2\}$ ,  $\boldsymbol{\epsilon} = \{\epsilon_1, \epsilon_2\}$ , and  $\boldsymbol{\delta} = \{\delta_1, \delta_2\}$  [17,18]. The Diophantine equation is  $n_1 q_1 + n_2 q_2 = 0$ . The  $t_0$ -averaged expectation value (13) can be written as

$$\begin{aligned} & \langle \langle \cos^k \theta \rangle \rangle(t, \epsilon_1, \epsilon_2, \delta_1, \delta_2) \\ &= \sum_{j=0}^{+\infty} |C_j(t, \epsilon_1, \epsilon_2)| (\epsilon_1^{q_2} \epsilon_2^{q_1})^j \cos[j\xi_{12} + \Theta_j(t, \epsilon_1, \epsilon_2)], \end{aligned} \quad (\text{B4})$$

where  $\xi_{12} = (q_1 \delta_2 - q_2 \delta_1)$  and  $\Theta_0(t, \epsilon_1, \epsilon_2) = 0$  [19]. Due to the inversion of the electric-field direction symmetry (17), it holds that (i) the series (B4) includes only even terms for  $k$

even if  $q_1 + q_2$  is odd, otherwise all the terms contribute; (ii) Eq. (B4) includes only odd ones for  $k$  odd if  $q_1 + q_2$  is odd; and (iii) if  $q_1 + q_2$  is even,  $\langle \langle \cos^k \theta \rangle \rangle = 0$  with  $k$  odd, and for  $k = 1$  the molecule is not oriented.

For  $H = H_0 + H_\mu + H_\alpha$ , six harmonics appear in the Hamiltonian,  $s = 6$ , and the nonzero solution of the Diophantine equation reads

$$(n_1 + 2n_3 + n_5 - n_6)q_1 + (n_2 + 2n_4 + n_5 + n_6)q_2 = 0, \quad (\text{B5})$$

and  $\mathbb{S} = \{n_1 = -2n_3 - n_5 + n_6 - mq_2, n_1 > 0, n_2 = -2n_4 - n_5 - n_6 + mq_1, (m, n_3, n_4, n_5, n_6) \in \mathbb{Z}^5\}$ . As a consequence,  $\mathbf{n} \cdot \boldsymbol{\delta} = m\xi_{12}$ . Using this result, Eq. (B2) can be rewritten as

$$\begin{aligned} & \langle \langle \cos^k \theta \rangle \rangle(t, \epsilon_1, \epsilon_2, \delta_1, \delta_2) \\ &= C_0(t, \epsilon_1, \epsilon_2) + \sum_{(n,m) \in \mathbb{S}} C_n(t, \epsilon_1, \epsilon_2) \epsilon_1^{|\mathbf{x}_n|} \epsilon_2^{|\mathbf{y}_n|} \\ & \quad \times \cos[m\xi_{12} + \Theta_n(t, \epsilon_1, \epsilon_2)], \end{aligned} \quad (\text{B6})$$

where  $x_n$ ,  $y_n$ , and  $m$  are integers determined not only by the solutions of the Diophantine equation, but also by the symmetries. Indeed, the symmetry (17) implies that  $|x_n| + |y_n|$  has the same parity as  $k$ . Thus, the expectation value (B6) is rewritten as

$$\begin{aligned} & \langle \langle \cos^k \theta \rangle \rangle(t, \epsilon_1, \epsilon_2, \delta_1, \delta_2) \\ &= \sum_{j=0}^{+\infty} C_j(t, \epsilon_1, \epsilon_2) \cos[j\xi_{12} + \varphi_j(t, \epsilon_1, \epsilon_2)], \end{aligned} \quad (\text{B7})$$

with  $C_j(t, -\epsilon_1, -\epsilon_2) = (-1)^k C_j(t, \epsilon_1, \epsilon_2)$ . Furthermore, due to the symmetry on the phases (16) two cases can be distinguished according to the parity of  $q_1 + q_2$ .

(i) If  $q_1 + q_2$  is an even integer,  $q_1$  and  $q_2$  are both odd integer numbers because  $\text{gcd}(q_1, q_2) = 1$ . As a consequence of the symmetry (16), it holds that  $\langle \langle \cos^k \theta \rangle \rangle = (-1)^k \langle \langle \cos^k \theta \rangle \rangle$ , and  $\langle \langle \cos^k \theta \rangle \rangle = 0$  for  $k$  odd, and  $\langle \langle \cos^k \theta \rangle \rangle$  satisfies (B7) for  $k$  even.

(ii) If  $q_1 + q_2$  is an odd integer,  $q_1$  and  $q_2$  have different parity. Due to the symmetry (16), for odd or even values of  $k$  in (B7), only odd or even terms contribute to the corresponding expansion, respectively, i.e.,

$$\begin{aligned} & \langle \langle \cos^{2k+1} \theta \rangle \rangle(t, \epsilon_1, \epsilon_2, \delta_1, \delta_2) \\ &= \sum_{\substack{j=1 \\ (j \text{ odd})}}^{+\infty} C_j(t, \epsilon_1, \epsilon_2) \cos[j\xi_{12} + \varphi_j(t, \epsilon_1, \epsilon_2)] \end{aligned} \quad (\text{B8})$$

and

$$\begin{aligned} & \langle \langle \cos^{2k} \theta \rangle \rangle(t, \epsilon_1, \epsilon_2, \delta_1, \delta_2) \\ &= \sum_{\substack{j=0 \\ (j \text{ even})}}^{+\infty} C_j(t, \epsilon_1, \epsilon_2) \cos[j\xi_{12} + \varphi_j(t, \epsilon_1, \epsilon_2)]. \end{aligned} \quad (\text{B9})$$

For  $H = H_0 + H_\mu + H_\alpha + H_\beta$ ,  $s = 14$  in the set of nonzero solutions (B3) of the Diophantine equation, which reads  $[n_1 + 2(n_3 + n_{11} - n_{12}) + n_5 - n_6 + n_7 + 3n_9 + n_{13} - n_{14}]q_1 + [n_2 + 2(n_4 + n_{13} + n_{14}) + n_5 + n_6 + n_8 + 3n_{10} + n_{11} + n_{12}]q_2 = 0$ . Therefore,  $\mathbb{S} = \{n_1 = -2(n_3 + n_{11} - n_{12}) - n_5 + n_6 - n_7 - 3n_9 - n_{13} + n_{14} - mq_2, n_1 > 0, n_2 = -2(n_4 + n_{13} + n_{14}) - n_5 - n_6 - n_8 - 3n_{10} - n_{11} - n_{12} + mq_1, (m, n_3,$

$n_4, \dots, n_{14}) \in \mathbb{Z}^{13}$ . As a consequence,  $\mathbf{n} \cdot \boldsymbol{\delta} = m\xi_{12}$  is also satisfied. In this case, expression (B6) is also obtained, and a similar symmetry analysis transforms it into the formula

(B7) if  $q_1 + q_2$  is an even integer, and if  $q_1 + q_2$  is odd into Eqs. (B8) and (B9). Finally, note that Eq. (B4) can also be rewritten as Eqs. (B8) and (B9) if  $q_1 + q_2$  is an odd integer.

- 
- [1] S. Flach, O. Yevtushenko, and Y. Zolotaryuk, *Phys. Rev. Lett.* **84**, 2358 (2000).
- [2] P. Reimann, *Phys. Rep.* **361**, 57 (2002).
- [3] M. Schiavoni, L. Sánchez-Palencia, F. Renzoni, and G. Grynberg, *Phys. Rev. Lett.* **90**, 094101 (2003).
- [4] S. Ooi, S. Savel'ev, M. B. Gaifullin, T. Mochiku, K. Hirata, and F. Nori, *Phys. Rev. Lett.* **99**, 207003 (2007).
- [5] P. Hänggi and F. Marchesoni, *Rev. Mod. Phys.* **81**, 387 (2009).
- [6] Y. Zolotaryuk and M. M. Osmanov, *Eur. Phys. J. B* **79**, 257 (2011).
- [7] D. Cubero, V. Lebedev, and F. Renzoni, *Phys. Rev. E* **82**, 041116 (2010).
- [8] N. R. Quintero, R. Alvarez-Nodarse, and J. A. Cuesta, *J. Phys. A: Math. Gen.* **44**, 425205 (2011).
- [9] K. Seeger and V. Maurer, *Solid State Commun.* **27**, 603 (1978).
- [10] A. V. Ustinov, C. Coqui, A. Kemp, Y. Zolotaryuk, and M. Salerno, *Phys. Rev. Lett.* **93**, 087001 (2004).
- [11] R. Gommers, S. Bergamini, and F. Renzoni, *Phys. Rev. Lett.* **95**, 073003 (2005).
- [12] A. Engel, H. W. Müller, P. Reimann, and A. Jung, *Phys. Rev. Lett.* **91**, 060602 (2003).
- [13] T. Salger, S. Kling, T. Hecking, C. Geckeler, L. Morales-Molina, and M. Weitz, *Science* **326**, 1241 (2009).
- [14] M. Salerno and Y. Zolotaryuk, *Phys. Rev. E* **65**, 056603 (2002).
- [15] L. Morales-Molina, N. R. Quintero, F. G. Mertens, and A. Sánchez, *Phys. Rev. Lett.* **91**, 234102 (2003).
- [16] N. R. Quintero, Soliton ratchets in sine-Gordon-like equations, in *The sine-Gordon Model and its Applications*, Nonlinear Systems and Complexity Vol. 10, edited by J. Cuevas-Maraver, P. Kevrekidis, and F. Williams (Springer, New York, 2014).
- [17] N. R. Quintero, J. A. Cuesta, and R. Alvarez-Nodarse, *Phys. Rev. E* **81**, 030102(R) (2010).
- [18] J. A. Cuesta, N. R. Quintero, and R. Alvarez-Nodarse, *Phys. Rev. X* **3**, 041014 (2013).
- [19] J. Casado-Pascual, J. A. Cuesta, N. R. Quintero, and R. Alvarez-Nodarse, *Phys. Rev. E* **91**, 022905 (2015).
- [20] K. von Meyenn, *Z. Physik* **231**, 154 (1970).
- [21] B. Friedrich and D. R. Herschbach, *Nature (London)* **353**, 412 (1991).
- [22] B. Friedrich and D. R. Herschbach, *Z. Phys. D* **18**, 153 (1991).
- [23] B. Friedrich, D. P. Pullman, and D. R. Herschbach, *J. Phys. Chem.* **95**, 8118 (1991).
- [24] M. J. Vrakking and S. Stolte, *Chem. Phys. Lett.* **271**, 209 (1997).
- [25] H. Stapelfeldt and T. Seideman, *Rev. Mod. Phys.* **75**, 543 (2003).
- [26] H. J. Loesch and A. Remscheid, *J. Chem. Phys.* **93**, 4779 (1990).
- [27] J. Bulthuis, J. Miller, and H. J. Loesch, *J. Phys. Chem. A* **101**, 7684 (1997).
- [28] H. Li, K. J. Franks, R. J. Hanson, and W. Kong, *J. Phys. Chem. A* **102**, 8084 (1998).
- [29] B. Friedrich and D. R. Herschbach, *J. Chem. Phys.* **111**, 6157 (1999).
- [30] B. Friedrich and D. Herschbach, *J. Phys. Chem. A* **103**, 10280 (1999).
- [31] H. Sakai, S. Minemoto, H. Nanjo, H. Tanji, and T. Suzuki, *Phys. Rev. Lett.* **90**, 083001 (2003).
- [32] S. Minemoto, H. Nanjo, H. Tanji, T. Suzuki, and H. Saka, *J. Chem. Phys.* **118**, 4052 (2003).
- [33] L. Holmegaard, J. H. Nielsen, I. Nevo, H. Stapelfeldt, F. Filsinger, J. Küpper, and G. Meijer, *Phys. Rev. Lett.* **102**, 023001 (2009).
- [34] J. H. Nielsen, H. Stapelfeldt, J. Küpper, B. Friedrich, J. J. Omiste, and R. González-Férez, *Phys. Rev. Lett.* **108**, 193001 (2012).
- [35] J. J. Omiste and R. González-Férez, *Phys. Rev. A* **86**, 043437 (2012).
- [36] C.-C. Shu, K.-J. Yuan, W.-H. Hu, and S.-L. Con, *J. Chem. Phys.* **132**, 244311 (2010).
- [37] S. Fleischer, Y. Zhou, R. W. Field, and K. A. Nelson, *Phys. Rev. Lett.* **107**, 163603 (2011).
- [38] K. Kitano, N. Ishii, and J. Itatani, *Phys. Rev. A* **84**, 053408 (2011).
- [39] M. Lapert and D. Sugny, *Phys. Rev. A* **85**, 063418 (2012).
- [40] C.-C. Shu and N. E. Henriksen, *Phys. Rev. A* **87**, 013408 (2013).
- [41] K. N. Egodapitiya, S. Li, and R. R. Jones, *Phys. Rev. Lett.* **112**, 103002 (2014).
- [42] T. Kanai and H. Sakai, *J. Chem. Phys.* **115**, 5492 (2001).
- [43] K. Oda, M. Hita, S. Minemoto, and H. Sakai, *Phys. Rev. Lett.* **104**, 213901 (2010).
- [44] P. M. Kraus, D. Baykusheva, and H. J. Wörner, *J. Phys. B* **47**, 124030 (2014).
- [45] P. M. Kraus, D. Baykusheva, and H. J. Wörner, *Phys. Rev. Lett.* **113**, 023001 (2014).
- [46] D. Baykusheva, M. S. Ahsan, N. Lin, and H. J. Wörner, *Phys. Rev. Lett.* **116**, 123001 (2016).
- [47] P. S. Pershan, J. P. van der Ziel, and L. D. Malmstrom, *Phys. Rev.* **143**, 574 (1966).
- [48] J. O. Hirschfelder, *Intermolecular Forces* (Interscience, New York, 1967).
- [49] A. J. Stone, *The Theory of Intermolecular Forces* (Clarendon, Oxford, 1996).
- [50] M. Beck, A. Jäckle, G. Worth, and H. D. Meyer, *Phys. Rep.* **324**, 1 (2000).
- [51] B. Deppe, G. Huber, C. Kränkel, and J. Küpper, *Opt. Express* **23**, 28491 (2015).
- [52] S. De, I. Znakovskaya, D. Ray, F. Anis, N. G. Johnson, I. A. Bocharova, M. Magrakvelidze, B. D. Esry, C. L. Cocke, I. V. Litvinyuk, and M. F. Kling, *Phys. Rev. Lett.* **103**, 153002 (2009).
- [53] G. Maroulis and M. Menadakis, *Chem. Phys. Lett.* **494**, 144 (2010).
- [54] J. H. Mun, H. Sakai, and R. González-Férez, *Phys. Rev. A* **99**, 053424 (2019).